

Formation and Properties of Model Crystalline Blends Comprising Diacetylene-Containing Polyester and Polyolefin. Tensile Behavior and Deformation Micromechanics

P. A. Lovell, J. L. Stanford, Y.-F. Wang, and R. J. Young*

Polymer Science and Technology Group, Manchester Materials Science Centre, UMIST/University of Manchester, Grosvenor Street, Manchester M1 7HS, UK

Received January 22, 1997; Revised Manuscript Received August 27, 1997

ABSTRACT: Model blends comprising a cross-polymerized diacetylene-containing polyester (PE) and poly[ethylene-co(vinyl acetate)] (EVA) were prepared and their mechanical properties evaluated. The dependence of the Young's modulus of the blends upon composition has been modeled by using a variety of theories for the deformation of multiphase polymers. Deformation of the cross-polymerized polyester phase in the blends was monitored by using Raman spectroscopy. The polyester phases within the blends produce well-defined Raman spectra in which the C≡C stretching bands undergo significant stress-induced band shifts during deformation of the blends. The results show that the Raman technique allows direct measurement of the stress in the polyester phase in a blend, independent of the overall deformation of the blend. Simultaneous deformation and Raman spectroscopy studies, therefore, give a unique insight into the deformation micromechanics of polymer blends.

Introduction

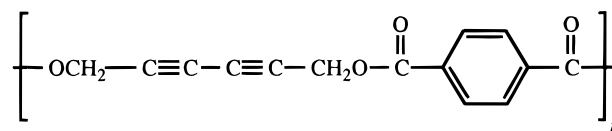
The mechanical properties of multiphase materials, such as copolymers, blends, and composites, depend strongly upon the efficiency of stress transfer between the phases during deformation of the materials. It is important, therefore, to be able to determine directly the stress/strain distribution within a particular component of a multiphase material during deformation. The direct determination of the micromechanics of deformation of model composites using Raman spectroscopy has now been reported.^{1–4} In these studies, Raman spectroscopy was used to monitor the micromechanics of deformation of high-performance fibers by mapping the stress-induced shifts in the Raman bands from point-to-point along individual fibers embedded in a resin matrix. The mechanical properties of these fiber-reinforced composites are controlled by the transfer of stress from the matrix to the fibers at the fiber/matrix interface⁵ and Raman spectroscopy has allowed a unique insight of this process to be obtained.^{2–4}

The mechanical properties of immiscible polymer blends are well known to be strongly affected by stress transfer between the phases in the blend.^{6–8} The present paper is one of a series^{9–12} concerned with the synthesis, structure, and properties of model polymer blends and an investigation of deformation micromechanics in the blends using Raman spectroscopy. One component in the blends is a polydiacetylene-containing phase for which it is possible to follow deformation using the stress-induced shift of the peak position of the Raman C≡C stretching band, as has been done for high-performance fibers in a polymer matrix. This approach was developed for the study of deformation processes in a series of urethane–diacetylene copolymers^{13–16} where the morphology was created by *in situ* phase separation during copolymerization. The present series of papers,^{9–12} however, represents the first attempt to use the technique to study the micromechanics of polymers blends.

This paper is concerned with an investigation into the relationship between the structure and mechanical properties of a series of blends.¹¹ The preparation, morphology and thermal properties of the blends investigated were described in detail in the preceding paper.¹²

Experimental Section

Materials Processing. The materials used in the present study were a diacetylene-containing polyester (PE) and blends of the polyester with poly[ethylene-co(vinyl acetate)] (EVA). The chemical repeat unit of the polyester PE is



(I)

and the details of the EVA and the preparation and properties of the PE have been described in detail in the preceding paper¹² and elsewhere.¹¹ The procedure used to prepare the four blends of the PE and EVA and the code numbers used to describe the blends are the same as in the preceding paper.¹² The resulting polymer blends were dried under vacuum to constant weight in the dark at room temperature prior to compression molding.

The four blends and their parent component polymers were compression molded into dumb-bells (overall dimensions 70 × 10 × 3 mm; gauge section 28 × 6 × 3 mm) and beams (70 × 10 × 3 mm) for mechanical testing according to the procedure described in the preceding paper.¹² During molding the materials which contained the PE attained the deep purple color characteristic of polydiacetylenes^{13–15} due to cross-polymerization¹² within the PE phases in the blends. All specimens were smoothed by using successively finer grades of metallographic grinding paper prior to testing.

Mechanical Testing. Tensile testing of the dumbbells was performed at 20 ± 3 °C on an Instron 1122 universal testing machine, equipped with a 0–2 kN load cell using a cross-head speed of 1 mm min^{−1} and an initial clamp separation of 28 mm. Strains up to 10% were measured independently using

* To whom correspondence should be addressed.

a 25-mm strain gauge extensometer which was clamped directly onto the parallel portion of the specimen. Strains above 10% were determined from the cross-head displacement. Six specimens were tested for each material and the average values of the derived tensile properties were obtained.

Simultaneous Tensile Testing and Raman Spectroscopy. Resonance Raman spectra of the cross-polymerized polyester powders were recorded by using a Raman microprobe system¹⁷ which is based on a Spex 1403 double-monochromator with a modified Nikon optical microscope attachment. A charge-coupled device (CCD), cooled with liquid nitrogen, was employed for signal detection and a 15-mW helium–neon laser (wavelength 632.8 nm) was used as the excitation source. A $\times 40$ objective lens with a numerical aperture of 0.65 was used and the laser, polarized in a direction parallel to the axis of tensile deformation, was focused on the sample to a spot of diameter $\sim 2 \mu\text{m}$. The scattered light was collected by using a 180° back-scattering geometry with the same objective lens and then focused on the entrance slit (~ 0.40 mm wide) of the spectrometer. Spectra over the wavenumber range 200–2200 cm^{-1} were obtained by splicing together spectral windows recorded in intervals of 40 cm^{-1} using a 10 s scanning time for each wavenumber interval. Spectral windows specific to the C=C and C≡C stretching vibrations were obtained in the same way, but in each case only three scans were required to define the specific local spectra. A nonlinear, least-squares fitting routine, based on the Levenberg–Marquardt algorithm,¹⁸ was used to fit peaks to a Gaussian function assuming a quadratic baseline curve. A resolution of $\pm 5 \text{ cm}^{-1}$ was usually achieved for the determination of the absolute values of the peak Raman wavenumber.

Raman spectra of the cross-polymerized model blends were obtained from the surfaces of the compression-molded rectangular bar specimens. The outer 50 μm of the surfaces were removed by grinding to eliminate any possible skin–core effects due to differences in thermal history between the skin and core regions of the specimens. The Raman spectra were recorded while the samples were deformed to fracture on a Minimat (Polymer Laboratories miniature mechanical tester). The deformation of the specimens was carried out stepwise under the Raman microprobe and the spectra were obtained immediately after each increment in deformation. Each Raman spectrum was recorded over a 10 s period. For blends containing low PE contents there was a possibility of stress relaxation due to the presence of the soft EVA matrix and this was examined by undertaking a loading/unloading/reloading experiment on B-40PE.

For the PE and B-80PE, deformation was carried out at a rate of 0.1 mm min^{-1} with a strain increment of about 0.004% for each step. For the other model blends, a deformation rate of 0.4 mm min^{-1} was used with a strain increment of 0.2% for each step. The overall strain on the bulk material was measured to an accuracy of $\pm 0.0014\%$ by using a resistance strain gauge which was attached to the specimen with M-Bond 200 adhesive (Micro-measurements Group Inc.).

Results and Discussion

Mechanical Properties. Tensile stress–strain curves and the derived tensile properties of the model blends and their pure components are presented in Figure 1 and Table 1. The values of tensile modulus (E) listed in Table 1 are the secant moduli at 0.1% elongation.

Figure 1 shows the wide range of mechanical behavior obtained as blend composition is changed. The materials exhibit properties which vary from those typical of a ductile plastic at low polyester contents, to those typical of a brittle plastic at high polyester contents. As well as the compositional change, this range of properties reflects the change in morphology as the polyester content is increased.¹² Figures 2 and 3 show the respective variations of tensile modulus (E), ultimate

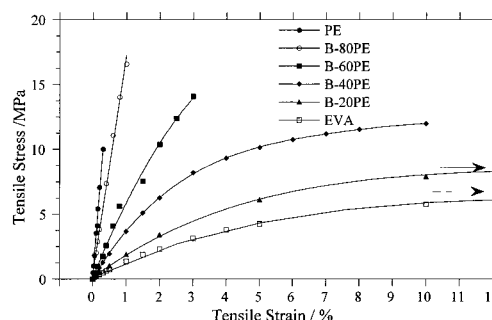


Figure 1. Tensile stress–strain curves for the cp-PE and EVA and the model blends listed in Table 1. Each data point is the average value of six measurements. (The horizontal arrows for B-20PE and EVA indicate continuing stress–strain curves with failure strains $> 12\%$.)

Table 1. Tensile Properties of the Polydiacetylene-Containing Polyester (PE), EVA, and PE/EVA Blends

material	$W_{\text{PE}},^a \%$	ϕ_{PE}^b	$E,^c \text{ MPa}$	$\sigma_u,^d \text{ MPa}$	$\epsilon_u,^e \%$
EVA	0	0	203 ± 5	10.4 ± 1.8	217 ± 10
B-20PE	20	0.17	303 ± 7	9.7 ± 0.7	41.8 ± 3.0
B-40PE	40	0.35	540 ± 10	12.3 ± 0.7	12.3 ± 1.6
B-60PE	60	0.55	980 ± 40	14.9 ± 0.9	2.9 ± 0.1
B-80PE	80	0.76	2020 ± 60	19.2 ± 0.8	1.1 ± 0.1
PE	100	1.00	3450 ± 40	8.9 ± 0.8	0.23 ± 0.05

^a Weight percentage of the polyester (PE) in blends. ^b Volume fraction of polyester in the model blends, which is calculated as $\phi_{\text{PE}} = (W_{\text{PE}}/\rho_{\text{PE}})/[(100 - W_{\text{PE}})/\rho_{\text{PVA}} + W_{\text{PE}}/\rho_{\text{PE}}]$, where ρ_{PE} is the density of PE ($\rho_{\text{PE}} = 1.128 \pm 0.004 \text{ g cm}^{-3}$) and ρ_{EVA} is the density of EVA ($\rho_{\text{EVA}} = 0.914 \pm 0.006 \text{ g cm}^{-3}$). ^c Tensile modulus is the secant modulus at 0.1% elongation. ^d Ultimate tensile stress. ^e Ultimate tensile strain.

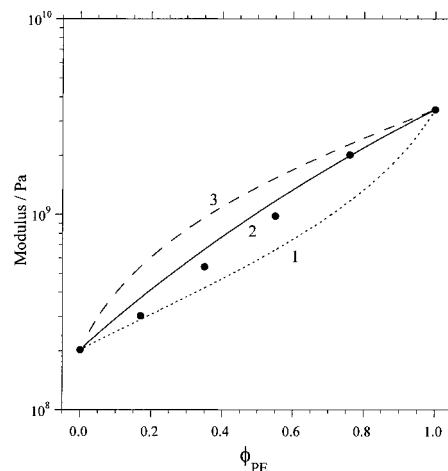


Figure 2. Semilog plot of Young's modulus versus volume fraction (ϕ_{PE}) of polyester (PE) for the model blends. The solid circles are experimental data. Curve 1 is the prediction of Kerner's equation²³ for a material with a rubbery matrix, curve 2 is the prediction of Davies' equation,²⁴ and curve 3 is the prediction of Kerner's equation²³ for a material with a glassy matrix.

tensile stress (σ_u), and ultimate tensile strain (ϵ_u) with the volume fraction (ϕ_{PE}) of cross-polymerized PE in the blends.

The model blends have values of tensile modulus between the extremes of the two pure components, as detailed in Table 1. The upper and lower bounds for the variation of modulus with blend composition (ϕ_{PE}) may be predicted simply by the Reuss and Voigt models.¹⁹ The Reuss model assumes that the elements in the blend (i.e., rigid cross-polymerized PE phase and

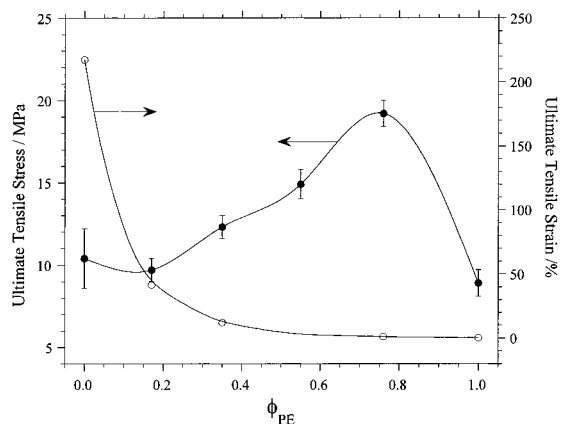


Figure 3. Variation of the ultimate tensile stress (σ_u) and ultimate tensile strain (ϵ_u) with the composition of the model blends, ϕ_{PE} .

soft EVA phase) act in series and experience the same stress. The Voigt model assumes that all the elements act in parallel and so experience the same strain. It was found that the experimental points fall between the Reuss and Voigt lines, indicating that the elements (i.e., two phases) do not act either in series or in parallel and the tensile moduli of the model blends cannot be predicted accurately by either the Reuss model or the Voigt models.

Other more sophisticated theories^{20–24} which have been developed to model the elastic properties of multiphase polymers have therefore been used to model the low-strain, elastic behavior of the model blends in terms of the moduli of each component and the blend composition. Figure 2 is a semi-log plot of Young's modulus versus ϕ_{PE} , the volume fraction of diacetylene-containing polyester PE in the model blends. Upper and lower bounds of the modulus of a two-phase blend are given by the modified Kerner equation,²³ which may be used to model the dependence of modulus upon composition for either glassy spheres in a continuous rubbery matrix and rubbery spheres in a continuous glassy matrix. Curves 1 and 3 are the solutions to the Kerner equation for rigid cp-PE in a continuous EVA phase and for EVA in a continuous rigid cp-PE phase, respectively. Another model, due to Davies,²⁴ uses an expansion of the theoretical treatment of the dielectric constant of two-phase materials to develop an expression, with no adjustable parameters, to predict the shear modulus of materials with two interpenetrating continuous phases (a co-continuous morphology). Although the theory was developed to model the shear modulus, there is no fundamental reason why it could not be used to predict the Young's modulus as well. According to Davies, the theory requires the existence of a perfect bond between the two phases, so that there is continuity of displacement across phase boundaries; curve 2 is a plot of the Davies equation. The theoretical Young's moduli were calculated by using values of the tensile modulus E of 203 MPa and a Poisson's ratio ν of 0.49 for EVA and values of 3.45 GPa for E and 0.35 for ν for the PE. The values of modulus are those measured for the two components separately and the values of Poisson's ratio assumed are typical of flexible (EVA) and rigid polymers (PE). Although Figure 2 shows that the modulus data for the model blends follow the same trends as the theoretical lines, it can be seen that none of the models can be used adequately to model the full modulus–composition behavior of the blends. This is due partly

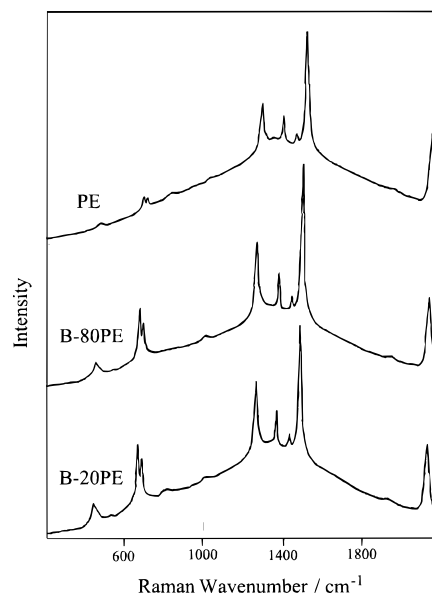


Figure 4. Typical Raman spectra of the pure polyester (PE) and the PE/EVA blends (B-80PE and B-20PE) showing the C≡C and C=C stretching bands at ~ 2100 cm⁻¹ and 1500 cm⁻¹ respectively, typical of a polydiacetylene.

to the complex phase structure¹² of the blends but the main problem is the lack of knowledge of the precise levels of stress in the different phases in the blends.

Figure 3 shows the dependence of both the ultimate tensile stress, σ_u , and ultimate tensile strain, ϵ_u , of the model blends as a function of PE volume fraction, ϕ_{PE} . It can be seen that ϵ_u decreases significantly as ϕ_{PE} increases reflecting the transition of the behavior of the blends from ductile to brittle. The dependence of σ_u upon ϕ_{PE} is more subtle, increasing first of all with increasing ϕ_{PE} and peaking at a polyester content of $\phi_{PE} \sim 0.8$ before decreasing rapidly for 100% polyester. The increase in σ_u with increasing ϕ_{PE} from 0.35 to 0.55 is due to the change in blend morphology from continuous–discontinuous (with EVA being the continuous phase) to a cocontinuous morphology.¹² The further increase in σ_u with increasing ϕ_{PE} from 0.55 to 0.76 is due to a phase-inversion¹² where the rigid cp-PE becomes the continuous phase with soft EVA as the dispersed phase, which may offer some toughening. The relatively low value of σ_u for the pure cross-polymerized PE is characteristic of a defect-sensitive brittle polymer.⁵

Deformation Studies Using Resonance Raman Spectroscopy. The Raman spectra of blends B-20PE and B-80PE at zero strain together with that of the cross-polymerized PE are shown in Figure 4. The assignment of the Raman bands was presented in a previous publication.¹¹ The spectra for the different materials in Figure 4 are virtually identical; the only significant changes that occur with the change in composition are in the intensity of the bands around 600 cm⁻¹.

It is well-established that the C≡C triple bond stretching band relative to other bands in the polydiacetylene cross-links has the highest sensitivity to deformation.^{13,15} Hence, this band was selected to monitor deformation in the polydiacetylene-containing polyester phase during deformation of the model blends. This was achieved by measuring the Raman shift factor, $d(\delta\nu)/d\epsilon$ (which is given in wavenumber shift of the Raman band peak per unit overall strain¹¹) for the cross-polymerized PE and the four blends.

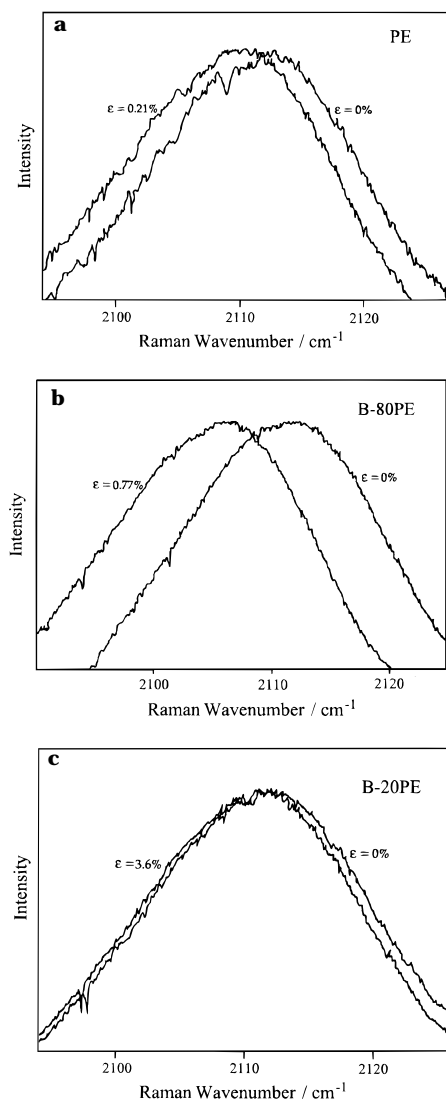


Figure 5. Raman spectra in the region of the C≡C triple bond stretching band showing the shift in the position of the band at the indicated overall strain (ϵ): (a) PE; (b) B-80PE; (c) B-20PE.

For each material, the C≡C Raman band was found to shift to lower wavenumber accompanied by slight band-broadening as the tensile deformation increased. Figure 5 shows some typical examples of this phenomenon for PE, B-80PE, and B-20PE. The shifts in band position clearly indicate that mechanical stress is transferred directly into deformation of the polydiacetylene cross-links in the polyester phase during the deformation of the model blends. The band broadening suggests that there is a distribution of stress and/or strain among the individual polydiacetylene chains. This distribution results from variations in local orientation of the polydiacetylene chains relative to the deformation axis of the tensile specimen. Similar observations and behavior have been made for diacetylene-containing segmented copolyurethanes.^{13–16}

The Raman wavenumber ($\Delta\nu$) at zero strain was found to vary by ± 1 cm⁻¹ from day-to-day due to a drift in instrument calibration but not during individual deformation experiments which were carried out over a period of 1–3 h. Hence, in order to make easy comparison of results obtained on different days, plots of Raman wavenumber shift ($\delta(\Delta\nu)$) for the C≡C band versus the overall tensile strain (ϵ) or stress (σ) are

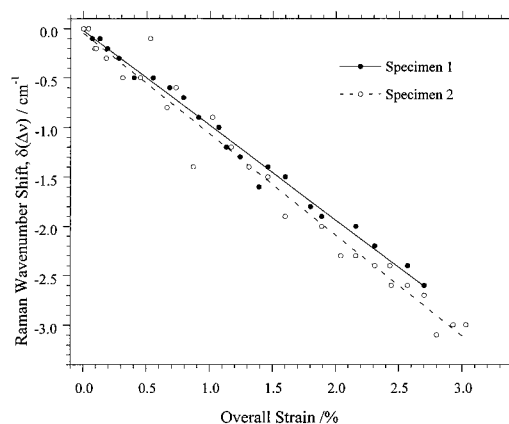


Figure 6. Strain-dependence of Raman wavenumber shift of C≡C the triple bond stretching band of two different molded specimens of the blend B-40PE.

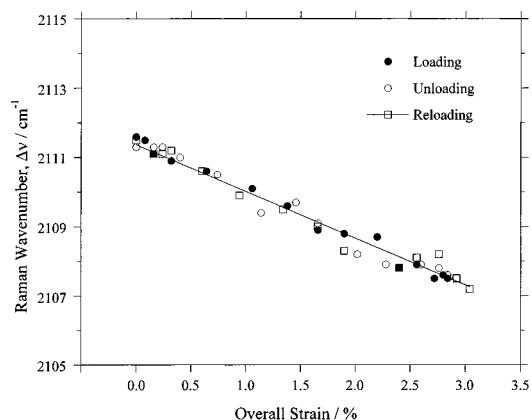


Figure 7. Plots of the Raman wavenumber of the C≡C triple bond stretching band versus the overall strain for the model blend B-40PE during cyclic loading.

plotted rather than plots of absolute Raman wavenumber. The Raman wavenumber shift ($\delta(\Delta\nu)$) was measurable to within ± 0.2 cm⁻¹. Figure 6 shows the linear relation between $\delta(\Delta\nu)$ and ϵ for two separately-molded specimens of blend B-40PE and demonstrates the reproducibility of the stress-induced Raman band shift measurements. This was a general observation for all materials studied.

For the blends containing low polyester contents, there is a possible stress relaxation during the stepwise deformation due to the viscoelastic nature of the soft EVA matrix. The extent of the stress relaxation can be examined by studying the reversibility of stress-induced Raman band wavenumber shifts. A loading–unloading–reloading cyclic loading test was carried out in the low strain (linear) region of the stress–strain curve (see Figure 1) for blend B-40PE. In this test, dumbbell specimens of blend B-40PE were stretched stepwise up to 3% strain and then unloaded gradually to 0% strain and stretched again, to 3% strain at the same rate. The Raman spectra were recorded after each deformation step. Figure 7 illustrates the relationship between the Raman band position and overall strain in the loading–unloading–reloading test and shows that for strains up to 3%, strain-induced Raman band shifts are completely reversible. This suggests that, although there is curvature in the tensile stress–strain curve for B-40PE in this strain range (see Figure 1), the blend shows complete elastic behavior and with no significant stress relaxation. It is anticipated, therefore, that

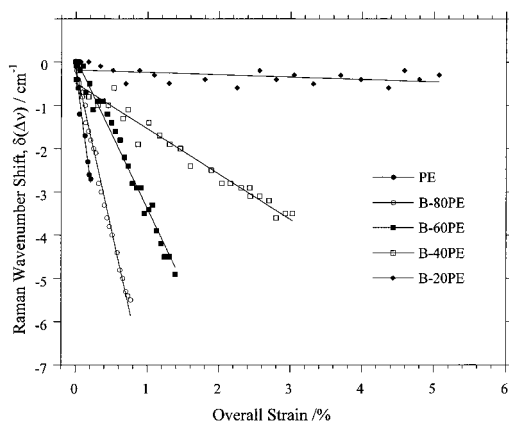


Figure 8. Strain-dependence of Raman wavenumber shift ($\delta(\Delta\nu)$) of the $\text{C}\equiv\text{C}$ triple bond stretching band of the PE and the model blend materials.

Table 2. Raman Shift Factors for $\text{C}\equiv\text{C}$ Stretching Band Positions in Polydiacetylene-Containing Model Blends^a

materials	$W_{\text{PE}},^b$ %	$E,^c$ MPa	$d(\delta(\Delta\nu))/d\epsilon,^d$ $\text{cm}^{-1}/\%$	$d(\delta(\Delta\nu))/d\sigma,^e$ $\text{cm}^{-1}/\text{MPa}$
PE	100	3450	-12.0 ± 0.3	-0.35
B-80PE	20	2020	-7.5 ± 0.4	-0.37
B-60PE	60	980	-3.5 ± 0.4	-0.36
B-40PE	40	540	-1.2 ± 0.3	-0.22
B-20PE	20	303	-0.1 ± 0.3	-0.03
diacetylene-containing copolyurethane ¹⁵	35 ^f	1660	-6.2 ± 0.4	-0.37
PUHD ²⁵ g		42000	-19.9	-0.047
TSHD ²⁶ g		50000	-20.3	-0.041
EUHD ²⁷ g		62000	-21.0	-0.034
DCHD ¹ g		45000	-19.7	-0.044

^a Comparative data for a diacetylene-containing copolymer and polydiacetylene single crystals are also included. ^b Weight percentage of polyester in the blends. ^c Tensile modulus quoted from Table 1. ^d The magnitude of the wavenumber shift per unit overall strain. ^e The magnitude of wavenumber shift per unit stress. ^f 35% by weight of diacetylene hard segments. ^g Polydiacetylene single crystals.

blends containing higher polyester contents (>40%) similarly will not experience stress relaxation during the stepwise deformation in Raman experiments. The above result demonstrates that stress-induced Raman band shifts are reversible and hence Raman spectroscopy can be used with confidence to study the deformation of the model blends.

Plots of the shift in Raman band wavenumber $\delta(\Delta\nu)$ versus the overall strain are shown in Figure 8 for all of the PE-containing materials studied. There is a linear relation between the Raman wavenumber shift ($\delta(\Delta\nu)$) and overall tensile strain (ϵ) for each of the materials studied, implying that the behavior of the materials is essentially Hookean over the range of strain investigated. The mean values of the Raman shift factor, $d(\delta(\Delta\nu))/d\epsilon$, for the $\text{C}\equiv\text{C}$ triple bond stretching band in each of the model materials were determined from at least three sets of data of $\delta(\Delta\nu)$ versus ϵ (cf. Figure 6) and the results are given in Table 2. The values of $d(\delta(\Delta\nu))/d\epsilon$ for the PE and PE blends are considerably lower than those for polydiacetylene single crystals (which have values of about $-20 \text{ cm}^{-1}/\%$ strain^{25–27}). Nevertheless, for blends with >80% PE the values of $d(\delta(\Delta\nu))/d\epsilon$ are higher than that for a diacetylene-containing copolyurethane (see Table 2).

It should be noted, however, that the Raman shift factor in terms of stress, $d(\delta(\Delta\nu))/d\sigma$, for PE is similar to that for the diacetylene-containing copolyurethane

and much higher than those for polydiacetylene single crystals (see Table 2). One possible explanation is that the local stress on the polydiacetylene chains in the PE and the copolyurethane is much higher than that in the polydiacetylene single crystals. This may be due to the fact that in the PE and the diacetylene-containing copolyurethane, the $\text{C}\equiv\text{C}$ bond is interconnected into a three-dimensional network and therefore undergoes three-dimensional deformation upon stretching. The network may lead to local stress concentrations upon the $\text{C}\equiv\text{C}$ bonds. In contrast, in the polydiacetylene single crystals, the $\text{C}\equiv\text{C}$ bond is in the linear backbone and only undergoes one-dimensional deformation upon stretching. There may also be a different polydiacetylene conjugation length for the molecules in the single crystal fibers. In fact, the cross-polymerized polyester PE can be treated mechanically as a three-dimensional randomly-distributed fiber-reinforced composite. In this case, the “fibers” are the extended polydiacetylene molecular chains although the Raman signal will come only from the chains aligned parallel to the direction of polarization of the laser light—i.e., the tensile axis.

According to the rule of mixtures for a three-dimensional randomly-distributed fiber-reinforced composite under a uniform-strain condition²⁸

$$E_{\text{cp PE}} = \eta_0 \eta_1 E_f V_f + E_{\text{PE}}(1 - V_f) \quad (1)$$

where $E_{\text{cp-PE}}$, E_f , and E_{PE} are the modulus of the cross-polymerized polyester PE, the polydiacetylene chains, and the polyester without cross-polymerization, respectively. V_f is the volume fraction of the polydiacetylene chains in the PE, which is estimated to be 0.10 from the chemistry of the solid-state cross-polymerization reaction and the degree of cross-polymerization.¹¹ η_0 is an orientation efficiency factor of the high-modulus polydiacetylene chains, equal to 0.2 for three-dimensional random distribution.²⁸ η_1 is a length correction factor, which may be taken as unity since the polydiacetylene backbones should have high aspect ratio.^{28,29} Assuming a value of $E_{\text{PE}} = 3 \text{ GPa}$ and using $E_{\text{cp-PE}} = 3.45 \text{ GPa}$, eq 1 is then satisfied by a value of $E_f = 40 \text{ GPa}$ for the modulus of the polydiacetylene chains in the PE, which is consistent with the typical value of 40–60 GPa²⁹ for polydiacetylene single crystals. Using this value of E_f the Raman wavenumber shift per unit local stress (σ_f) on the polydiacetylene chains in cp-PE, $d(\delta(\Delta\nu))/d\sigma_f$, is equal to $-0.03 \text{ cm}^{-1} \text{ MPa}^{-1}$, which is similar to the values for polydiacetylene single crystals (between -0.034 and $-0.047 \text{ cm}^{-1} \text{ MPa}^{-1}$, see Table 2).

Relationship between Raman Band Shifts and Blend Structure. Figure 9 shows that the Raman shift factors, $d(\delta(\Delta\nu))/d\epsilon$, of the blends determined from the increases in slopes of the lines in Figure 8 with increasing polyester content (W_{PE}). Figure 8 indicates that although the proportion of external tensile stress transferred directly into deformation of the polydiacetylene chains increases with increasing polyester content, it does not do so linearly. The rate of increase of $d(\delta(\Delta\nu))/d\epsilon$ with W_{PE} can be seen by taking the differential of $d(\delta(\Delta\nu))/d\epsilon$ with respect to W_{PE} and plotting against W_{PE} . This is shown by the dashed curve in Figure 9, from which it is evident that the largest change in “rate” is between 40 and 60% PE. This may be attributed to a significant change in morphology within this composition range. For blends with polyester contents from 20 to 40%, the PE is dispersed into the matrix EVA phase; for blends with polyester contents of 60%, the micro-

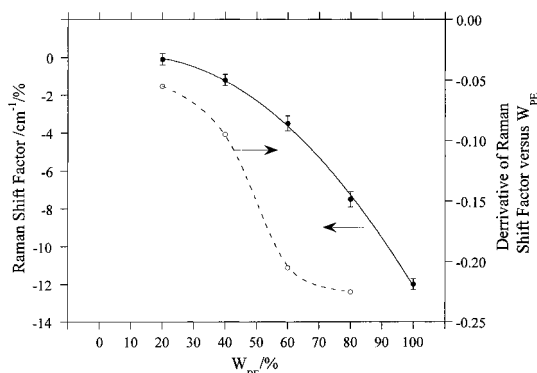


Figure 9. Effect of blend composition, W_{PE} , upon the Raman shift factor, $d(\delta(\Delta\nu))/d\epsilon$.

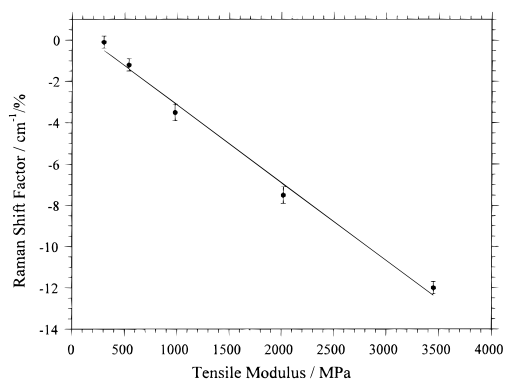


Figure 10. Plot of Raman shift factor, $d(\delta(\Delta\nu))/d\epsilon$, versus tensile modulus (E) for the model materials studied.

structure is cocontinuous and for 80% polyester the cp-PE is the continuous phase.¹²

Figure 10 shows a plot of the Raman shift factors, $d(\delta(\Delta\nu))/d\epsilon$, versus the tensile modulus, E , for the model materials. There is an approximately linear relationship between the Raman shift factor and the tensile modulus for the materials studied, indicating that the stress-induced Raman shift factor is proportional to the tensile modulus of the model materials. The apparently linear relationship results from the monotonic but nonlinear relationships for both plots of $d(\delta(\Delta\nu))/d\epsilon$ versus composition (Figure 9) and E versus composition (Figure 2). One possible explanation for this linear relationship might be that the diacetylene-containing polyester phase experiences higher local stress (σ_{PE}) for the higher-modulus model blends, and the local stress (σ_f) transferred directly into the deformation of polydiacetylene chains is proportional to the modulus of the model materials.

It is interesting to note that a proportional relationship is also found between $d(\delta(\Delta\nu))/d\epsilon$ and Young's modulus E for other systems with completely different structures such as aramid fibers³⁰ and carbon fibers.³¹ This is consistent with the Raman shift factor $d(\delta(\Delta\nu))/d\epsilon$ being dependent upon the level of molecular stress (as opposed to strain) for both the aramid and carbon fibers and for the model blends investigated in this present study.

Strain Analysis of the PE Phase in the Model Blends. The stress-induced Raman wavenumber shift in the polydiacetylene-containing polyester and its model blends gives a unique insight into the micromechanics of deformation in the polydiacetylene-containing PE phase in relation to the overall deformation of the model blends. Raman spectroscopy is used as an optical

stress-probe to monitor the deformation of the polydiacetylene chains which are formed *in situ* in the crystalline domains of the diacetylene-containing polyester phase.

The study of polydiacetylene single crystal fibers using Raman spectroscopy has revealed^{26,29,32} that the strong Raman scattering in such single crystal fibers is obtained only when the direction of the laser polarisation is parallel to the axis of the polydiacetylene molecules (i.e., parallel to the fiber axis). For the deformation of isotropic polydiacetylene-containing copolyurethanes, it was observed³³ that the strain measured by Raman spectroscopy depends upon the angle (θ) of the polarization of the laser beam with respect to the tensile axis and decreases dramatically with increasing θ . This indicates that in the polydiacetylene-containing polyester and its model blends, the Raman signal comes mainly from the polydiacetylene chains that are oriented parallel to the polarization direction of the laser beam, which is the stretching direction in the present deformation experiments. Therefore, the stress-induced Raman wavenumber shift is largely attributed to the polydiacetylene chains aligned parallel to the deformation axis, implying that the Raman spectroscopy mainly probes the deformation of these molecular chains. Nevertheless, in terms of local strain, ϵ_f , on the polydiacetylene chains the Raman shift factor of the polydiacetylene chains, $d(\delta(\Delta\nu))/d\epsilon_f$, will be a constant as long as the chain orientation and the chain modulus E_f remain constant in all model materials studied; therefore, there is a linear relationship between the local strain ϵ_f on the polydiacetylene chains and the vibrational wavenumber of the C≡C stretching Raman band in all model materials studied here. Thus, the relationship between the Raman band wavenumber and the external tensile strain in the polydiacetylene-containing polyester (PE) has been used to evaluate the strain generated in the polydiacetylene-containing phase in the model blends. The strain in the rigid diacetylene-containing polyester PE phase in the model blend, ϵ_{PE} , can be calculated by taking the ratio of the Raman wavenumber shift ($\delta(\Delta\nu)_\epsilon$) of the model blend at overall strain ϵ to the Raman shift factor of polydiacetylene-containing polyester, $(d(\delta(\Delta\nu))/d\epsilon)_{cp-PE}$, using

$$\epsilon_{PE} = \frac{(\delta(\Delta\nu))_\epsilon}{(d(\delta(\Delta\nu))/d\epsilon)_{cp-PE}} \quad (2)$$

where ϵ_{PE} , $(d(\delta(\Delta\nu))/d\epsilon)_{cp-PE}$, and $(\delta(\Delta\nu))_\epsilon$ are the local strain in the PE phase, the Raman shift factor of PE, and the Raman band wavenumber shift of the model blend at the overall tensile strain ϵ , respectively. Plots of ϵ_{PE} versus ϵ for the model blends are shown in Figure 11a. Also, assuming that the tensile modulus of the PE phase in each of the blends is identical to the tensile modulus, E_{cp-PE} , of pure cross-polymerized PE, the local stress, σ_{PE} , in the cross-polymerized PE phase can be calculated from

$$\sigma_{PE} = \left[\frac{(\delta(\Delta\nu))_\epsilon E_{cp-PE}}{(d(\delta(\Delta\nu))/d\epsilon)_{cp-PE}} \right] \quad (3)$$

A plot of σ_{PE} versus overall strain for each blend is presented in Figure 11b.

Figure 11a,b shows that the local strain (ϵ_{PE}) and local stress (σ_{PE}) distributed in the cp-PE phase increase with increasing polyester content. For blend B-20PE, ϵ_{PE} is

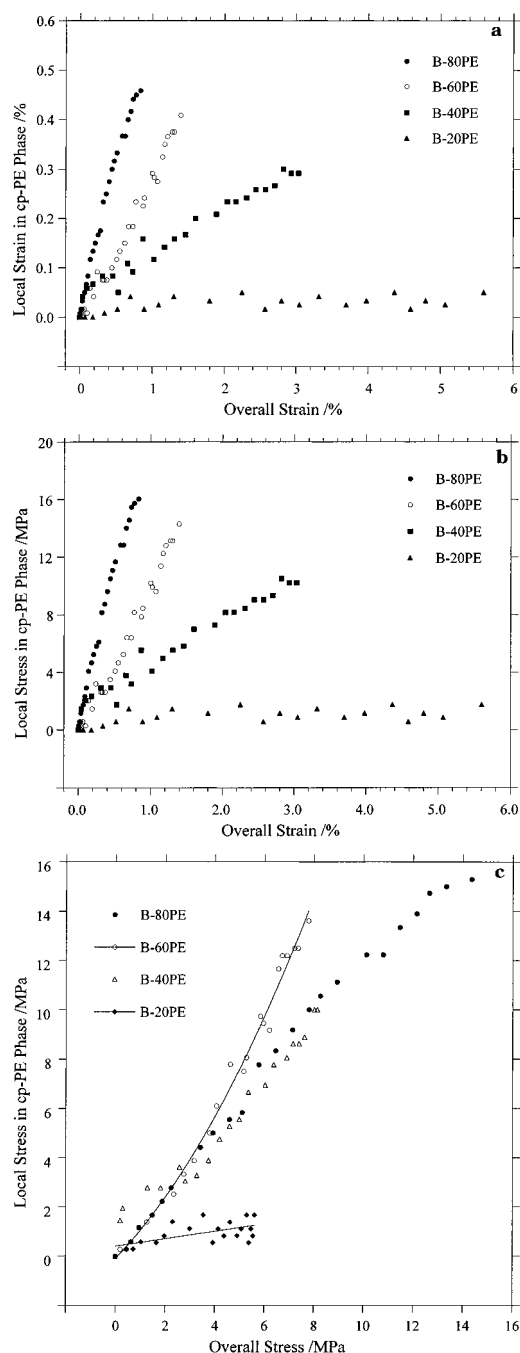


Figure 11. Stress-strain distributions within the diacetylene-containing PE phase of the blends. (a) Plots of local strain, ϵ_{PE} , in the rigid PE phase against the overall strain, ϵ , of the model blends during deformation. (b) Plots of local stress, σ_{PE} , in the rigid PE phase against the overall strain, ϵ , of the model blends during deformation. (c) Plots of local stress, σ_{PE} , in the rigid PE phase against the overall stress, σ , of the model blends during deformation.

very small compared with the overall strain and the contribution of the PE phase to the overall deformation of the blends is negligible; the dispersed PE phase experiences only very low stress. For blend B-40PE ϵ_{PE} and σ_{PE} are much higher than those for blend B-20PE indicating better stress transfer, although ϵ_{PE} still represents only a small fraction (about 10%) of the overall strain. The ϵ_{PE} for blend B-60PE is about 30% of the overall strain and the ϵ_{PE} for blend B-80PE is about 60% of the overall strain and the PE phases experience very high local stress σ_{PE} ; i.e., there are much

higher contributions from deformation of the PE phase to the overall strain for blends B-60PE and B-80PE than for blends B-20PE and B-40PE. This is consistent with the observation that the PE phases in blends B-60PE and B-80PE are cocontinuous and continuous¹² and therefore experience a much higher proportion of strain than in B-20PE and B-40PE. In addition, it is interesting to note that, except for blend B-20PE in which poor bonding exists between the two phases,¹² the local stress σ_{PE} is equal to or higher than overall stress (see Figure 11c). This is particularly significant for blend B-60PE which has a cocontinuous phase morphology. It is significant to note that the high values of σ_{PE} for the blends imply that the PE phase is offering considerable reinforcement. This unique insight is only possible through the use of Raman spectroscopy to follow deformation processes.

The above Raman deformation experiments have shown conclusively that the phases in the blend are under conditions of neither uniform stress nor uniform strain and support the earlier observation that simple mechanical models such as Reuss and Voigt averages¹⁹ cannot be used successfully to model the mechanical behavior of the blends.

Conclusions

The diacetylene-containing polyester PE is a brittle polymer with a tensile modulus of 3.45 GPa. Tensile stress-strain curves of the diacetylene-containing model blends show both ductile and brittle failure depending on blend composition. A value of 40 GPa is calculated for the polydiacetylene chains in the crystalline domains of PE by using the rule of mixtures prediction for a fiber-reinforced composite containing a three-dimensional distribution of discontinuous fibers.

The C≡C triple bond stretching Raman band in the polydiacetylene-containing polyester PE and its model blends shifts to lower wavenumber during tensile deformation. For the pure PE, shifts of -12.0 cm^{-1} per % strain or $-0.35 \text{ cm}^{-1} \text{ MPa}^{-1}$ are obtained, and for the blends the shifts depend on the blend composition and increase from -0.1 to -7.5 cm^{-1} per % strain as PE content increases from 20 to 80%. The local stress σ_{PE} and strain ϵ_{PE} in the polydiacetylene-containing polyester PE phase in the model blends were calculated by taking the ratio of the Raman wavenumber shift of the model blend at overall strain ϵ to the Raman shift factor of the PE. The data show clearly that the stress on the PE phase increases as the PE content increases. In particular, for a given overall strain on the blend, there is a major increase in the stress within the PE phase as the blend composition changes from 40 to 60% PE, corresponding to the transition from a discontinuous to a cocontinuous morphology.

The results demonstrate clearly that Raman spectroscopy can be used to probe the local stress and strain in the diacetylene-containing polyester phases of the model blends independent of the measurement of overall stress and strain, giving a unique insight into the deformation micromechanics.

Acknowledgment. Financial support for the research work reported in this paper was kindly provided by Exxon Chemical. R.J.Y. is grateful to the Royal Society for support in the form of the Wolfson Research Professorship in Materials Science.

References and Notes

- (1) Young, R. J.; Galiotis, C.; Robinson, I. M.; Batchelder, D. N. *J. Mater. Sci.* **1987**, *22*, 3642.
- (2) Bannister, D. J.; Andrews, M. C.; Cervenka, A. J.; Young, R. J. *Comp. Sci. Technol.* **1995**, *53*, 411.
- (3) Andrews, M. C.; Young, R. J. *J. Mater. Sci.* **1995**, *30*, 5607.
- (4) Andrews, M. C.; Day, R. J.; Young, R. J. *Comp. Sci. Technol.* **1993**, *48*, 255.
- (5) Kelly, A.; MacMillan, N. H. *Strong Solids* 3rd ed.; Clarendon Press: Oxford, 1986.
- (6) Paul, D. R., Newman, S., Eds. *Polymer Blends*; Academic Press: New York, 1978.
- (7) Utracki, L. A. *Polymer Alloys and Blends*; Hanser: Munich, 1989.
- (8) Folkes, M. J.; Hope, P. S. *Polymer Blends and Alloys*; Blackie: Glasgow, 1993.
- (9) Lovell, P. A.; Stanford, J. L.; Wang, Y.-F.; Young, R. J. *Macromol. Rep.* **1994**, *A31*, 811.
- (10) Lovell, P. A.; Stanford, J. L.; Wang, Y.-F.; Young, R. J. *Polym. Bull.* **1993**, *30*, 347.
- (11) Lovell, P. A.; Stanford, J. L.; Wang, Y.-F.; Young, R. J. *Polym. Int.* **1994**, *34*, 23.
- (12) Lovell, P. A.; Stanford, J. L.; Wang, Y.-F.; Young, R. J. *Macromolecules* **1998**, *31*, 834.
- (13) Day, R. J.; Stanford, J. L.; Young, R. J. *Polymer* **1991**, *32*, 1713.
- (14) Day, R. J.; Hu, X.; Stanford, J. L.; Young, R. J. *Polym. Bull.* **1991**, *27*, 353.
- (15) Hu, X.; Stanford, J. L.; Day, R. J.; Young, R. J. *Macromolecules* **1992**, *25*, 672 & 684.
- (16) Hu, X.; Stanford, J. L.; Day, R. J.; Young, R. J. *J. Mater. Sci.* **1992**, *27*, 5958.
- (17) Young, R. J. *J. Textile Institute* **1995**, *86*, 360.
- (18) Marquardt, D. W. *J. Soc. Ind. Appl. Math.* **1963**, *11*, 431.
- (19) Young, R. J.; Lovell, P. A. *Introduction to Polymers*; 2nd ed.; Chapman & Hall: London, 1991.
- (20) Dickie, R. A. In *Polymer Blends*; Paul, Newman, Eds.; Academic Press: New York, 1978; Vol. 2, Chapter 8.
- (21) Ryan, A. J.; Stanford, J. L.; Still, R. H. *Polymer* **1991**, *32*, 1426.
- (22) Tomlins, P. E.; Read, B. E. *Plast. Rubber Composites, Process. Appl.* **1991**, *16*, 17.
- (23) Kerner, E. H. *Proc. Phys. Soc. Lond. (B)* **1956**, *69*, 808.
- (24) Davies, W. E. *J. Phys. (D) Appl. Phys.* **1971**, *161*, 318, 1176, 1325.
- (25) Mitra, V. K.; Risen, W. M.; Baughman, R. H. *J. Chem. Phys.* **1977**, *66*, 731.
- (26) Batchelder, D. N.; Bloor, D. *J. Polym. Sci., Polym. Phys. Ed.* **1979**, *17*, 569.
- (27) Galiotis, C.; Young, R. J.; Batchelder, D. N. *J. Polym. Sci., Polym. Phys. Ed.* **1983**, *21*, 2483.
- (28) Hull, D. *An Introduction to Composite Materials*; Cambridge University Press: Cambridge, 1981; Chapter 5.
- (29) Young, R. J. In *Polymer Single Crystal Fibers in Developments in Oriented Polymers-2*; Ward, I. M., Ed.; Elsevier: London, 1987.
- (30) Young, R. J.; Lu, D.; Day, R. J.; Knoff, W. F.; Davies, H. A. *J. Mater. Sci.* **1992**, *27*, 5431.
- (31) Huang, Y.; Young, R. J. *Carbon* **1995**, *33*, 97.
- (32) Wu, G.; Tashiro, K.; Kobayashi, M. *Macromolecules* **1989**, *22*, 188.
- (33) Hu, X.; Stanford, J. L.; Young, R. J. *Polymer* **1994**, *35*, 81.

MA970072J